Polyethylene glycol and polyvinylpyrrolidone: potential green corrosion inhibitors for copper in H_2SO_4 solutions

N.T. Talat,[1]* A.A. Dahadha,[2] M. Abunuwar,[3] A.A. Hussien[1] and Wafa'a Odeh[4]

[1]Department of Mechanical, Faculty of Engineering, Al-Huson University College, Al-Balqa Applied University, P.O. Box 21510 (50), Irbid, Jordan
[2]Department of Biotechnology and Genetic Engineering, Faculty of Science, Philadelphia University, P.O. Box 19392, Amman, Jordan
[3]Faculty of Pharmacy, Philadelphia University, P.O. Box 19392, Amman, Jordan
[4]Department of Allied Medical Sciences, Al-Zarqa University College, Al-Balqa Applied University, Alzarqa, Jordan
E-mail: n.talat@bau.edu.jo

Abstract

Weight-loss, thermometric, and electrical conductance techniques were employed for the investigation of the influence of polyethylene glycol 400, 4000, and polyvinylpyrrolidone K15 as cost-effective, efficient, and eco-friendly inhibitors on the corrosion inhibition of copper in H_2SO_4 solution. The corrosion rates of copper in H_2SO_4 solutions increase with an increase in acid concentrations and temperatures in the absence of inhibitors. The addition of PEG 400, PEG 4000, and PVP K15 to the corrosive solutions was found to have a considerable inhibitory influence on the corrosion rates of copper at various temperatures. Consequently, the inhibition efficiency of PEG 400, PEG 4000 and PVP K15 increases with an increase in their concentrations. Remarkably, PVP K15 was a more efficient inhibitor than PEG 400, and PEG 4000, this effect might be attributed to the nature of the functional groups and the size of the PVP K15 chains. An evaluation of the temperature effect was studied to show that rising temperatures lead to an increased corrosion rate and lower inhibition efficiencies. However, PEG 400, PEG 4000, and PVP K15 inhibited copper corrosion by virtue of adsorption, which was found to accord with the Langmuir and Temkin adsorption isotherm models. Moreover, the thermodynamic aspects (ΔH^0, ΔS^0 and E_a) of the adsorption process were calculated and discussed.

Received: November 15, 2022. Published: March 7, 2023 doi: 10.17675/2305-6894-2023-12-1-13

Keywords: *corrosion inhibitor, copper, polyethylene glycol, polyvinylpyrrolidone, Temkin and Langmuir adsorption isotherms.*

1. Introduction

Copper and its alloys have a broad range of applications owing to their good properties such as conductivity, workability, and resistance, which make them a suitable choice for the manufacture of wires, thick/thin sheets, and electrical/electronic instruments. In addition,

they play a vital role in the car industry, oil refineries, sugar factories, and the marine environment [1]. As a result, copper alloys must be cleaned on a regular basis to descale these systems, and they will be exposed to an acidic corrosive environment during the cleaning process [2–4]. Many researchers have used a wide range of organic corrosion inhibitors that contain π-system and/or O, N, P, or S heteroatoms to reduce damage in corrosive environments [5, 6]. For example, Munoz *et al*. investigated the effect of three various inorganic inhibitors (chromate CrO_4^{2-}, molybdate MoO_4^{2-}, and tetraborate $B_4O_7^{2-}$) on the inhibition of the corrosion rate of copper in LiBr solution [7]. Gerengi and his group reported that benzotriazole has a significant role in the inhibition of copper corrosion in artificial seawater [8]. Similarly, Lee and colleagues demonstrated imidazole's inhibition influence as a powerful inhibitor of copper corrosion in a 1.0 mol·dm^{-3} HNO_3 solution [9]. Matjaz Finšgar used 2-mercaptobenzimidazole as an efficient copper corrosion inhibitor in a 3.0 wt.% aqueous NaCl solution, employing 3D-profilometry, electrochemical impedance spectroscopy, and potentiodynamic curve measurements to detect its efficiency [10].

On the other hand, recently, plant extracts have attracted more attention as powerful green corrosion inhibitors for several metals. In this field, Y.M. Abdallah *et al*. have utilized *Euphorbia helioscopia Linn* extract as a green inhibitor of copper corrosion in a 1.0 mol·dm^{-3} HNO_3 solution [11]. H.T. Rahal and his group studied the corrosion inhibition effects of plant leaf extracts, such as *Crataegus oxyacantha* (Hawthorn) and *Prunus avium* (Sweet Cherry), on the corrosion of mild steel in a 0.5 M HCl solution [12]. R.S. Al-Moghrabi *et al*. used willow (Salix) plant leaf extract to reduce the corrosion of mild steel in 0.5 M HCl and 0.5 M HNO_3 solutions [13]. A.M. Abdel-Gaber and colleagues investigated the inhibition effect of *Eucalyptus* plant leaf extract on mild steel corrosion in acidic mediums [14]. H.T. Rahal *et al*. found that *Fragaria ananassa* (Strawberry) and *Cucurbita pepo* L. (Zucchini) leaf extracts behave as efficient corrosion inhibitors of mild steel in HCl solutions [15]. K.M. Hijazi *et al*. investigated the inhibitive effect of sumac, *Rhus Coriaria* (RC) on corrosion of mild steel in 0.5 M of hydrochloric acid and sulfuric acid solutions using various techniques, like Atomic Force Spectroscopy (AFM), Electrochemical Impedance Spectroscopy (EIS), and Fourier Transform Infrared Spectroscopy (FTIR) [16].

Polyethylene glycols and polyvinylpyrrolidone are playing a significant role as green catalysts in multicomponent, oxidation-reduction and synthetic organic reactions due to their bio-compatibility, non-toxicity, low cost, recyclability, biodegradability and high thermal stability [17–23]. In addition, polyethylene glycol and polyvinylpyrrolidone were efficiently employed as green corrosion inhibitors. For instance, Ashassi-Sorkhabi and his colleague demonstrated the inhibition effect of various polyethylene glycols on carbon steel corrosion in sulfuric acid, where the efficiency of inhibition increases with increasing concentrations and molecular weights of polyethylene glycols [24]. Praveen *et al*. used polyethylene glycols as corrosion inhibitors for lead and lead-free solders in a 1.0 N HCl solution and found that the inhibition efficiency increased as the polyethylene glycol concentration increased [25]. While Nasr-Esfahani *et al*. used a mixture of polyethylene glycol and imidazole (PEG/IMZ)) to inhibit carbon steel in a 0.5 M H_2SO_4 solution, the efficiency of inhibition

increased with increasing temperature [26]. Al Juhaiman *et al*. used polyvinyl pyrrolidone as an efficient corrosion inhibitor for carbon steel in NaCl solutions [27]. Layla A. Al Juhaiman used polyvinylpyrrolidone carbon steel in an HCl solution to report that the inhibition efficiency of PVP increased significantly as PVP and temperature increased [28].

Therefore, the major target of the current work is to explore the inhibiting influence of some water-soluble polymers as low-cost, nontoxic, and eco-friendly corrosion inhibitors, namely polyethylene glycols (PEG 400 and 4000) and polyvinylpyrrolidone K15 (PVP K15), on the corrosion of copper in various concentrations of H_2SO_4 solutions by the use of gravimetric, thermodynamic, and electrical conductance techniques at 25–55°C. To the best of our knowledge, no studies have reported the use of electrical conductance as a simple, available, and efficient method to investigate the corrosion inhibition of copper.

2. Experimental

The copper samples (1.20 cm×1.20 cm) have been mechanically cut from commercially pure copper (Cu 99.5%) at 1.00 mm thick. They were polished with emery paper down to grade 600, then degreased with acetone and rubbed with a cotton rag. The samples have been dried in an oven to be stored in moisture-free desiccators before use in the corrosion studies. Stock solutions of 2.0, 1.5, 1.0, and 0.50 mol·dm^{-3} of sulfuric acid (95–97%; Sigma-Aldrich, USA) were prepared using the appropriate amounts of H_2SO_4 dissolved in doubly distilled water. In the same manner, solutions of 0.001 mol·dm^{-3} of each polyethylene glycol 400 (PEG 400) (Schariau, Spain) and 0.001 mol·dm^{-3} polyethylene glycol 4000 (PEG 4000) (Schariau, Spain) and polyvinylpyrrolidone (PVP K15) (with an approximate molecular weight of 10,000 g·mol^{-1}; Appli Chem, Germany) were made at the moment of their use. The study was carried out at 25–55°C with the help of a thermostated water bath.

2.1. Gravimetric measurements

In gravimetric measurements, four copper samples were completely immersed in 2.0, 1.5, 1.0, and 0.5 mol·dm^{-3} of H_2SO_4 solutions without inhibitors at 25, 35, 45, and 55°C. In each case, after 15.0 hours, the samples were taken out and washed in ethanol and water. However, the weight loss was accurately evaluated in mg for each copper sample at a specific temperature by calculating the difference between the initial weight and the weight after the removal of the corrosion product using a digital analytical balance with a precision of 0.0001 g, as shown in table 1S–4S. Each measurement was repeated three times under the same conditions to guarantee the reliability of the results, and an average value was reported. Weight loss was employed to estimate the corrosion rate using the following formula [29]:

$$\text{Corrosion rate} = \frac{534W}{\rho At} \tag{1}$$

where W is the weight loss (g), ρ is the density of the copper (g/cm^3), A is the area of the copper sample (cm^2), and t is the exposure time (h). To explore the effect of PEG 400,

PEG 4000, and PVP K15 as green corrosion inhibitors, the previous procedure was applied using (7.70×10^{-5}, 1.53×10^{-4}, 2.30×10^{-4}, and 3.07×10^{-4} mol·dm^{-3}) of PEG 400, PEG 4000, and PVP K15 in a 2.0 mol·dm^{-3} H_2SO_4 solution, as shown in table 6S–16S. The inhibition efficiency of the inhibitors in a 2.0 mol·dm^{-3} H_2SO_4 solution was evaluated using the following expression [29, 30] as illustrated in figures 1S–3S:

$$I(\%) = \left[1 - \frac{W_f}{W_i}\right] \times 100\% \quad (2)$$

where, W_i and W_f are the weight losses of the copper samples in the absence and presence of the corrosion inhibitors, respectively, in a 2.0 mol·dm^{-3} H_2SO_4 solution at the specific temperature. The degree of surface coverage (θ) was also calculated from equation (3):

$$\theta = 1 - \frac{W_f}{W_i} \quad (3)$$

3. Results and Discussion

3.1. Effect of H_2SO_4 concentration and temperature on the corrosion rate

The corrosion rate of copper in various concentrations of H_2SO_4 solution at 25–55°C in the absence of inhibitors was tested. Figure 1 exhibits the relationship between the corrosion rate versus concentrations of H_2SO_4 solutions at all temperatures. The corrosion rate of copper, on the other hand, increases as the concentration of H_2SO_4 solution increases. Figure 1 also shows that the corrosion rate of copper increases with increasing temperature. Noteworthy, the maximum corrosion rate for copper was achieved in a 2.0 mol·dm^{-3} of H_2SO_4 solution at 55°C. This observation might be attributed to the fact that the rates of chemical reactions often increase with an increase in the concentration of reactants, temperature, and time.

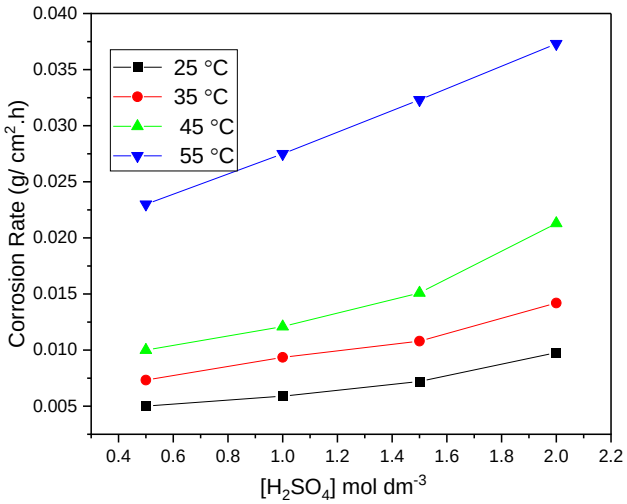

Figure 1. The corrosion rate of copper against various [H_2SO_4] at different temperatures.

3.2. Effect of inhibitors concentration and temperature on the inhibition efficiency

Figures 2–4 illustrate the plots of copper corrosion rates against different concentrations of PEG 400, PEG 4000, and PVP K15 solutions in a 2.0 mol·dm^{-3} H_2SO_4 solution at 25–55°C. Generally, PEG 400, PEG 4000, and PVP K15 inhibit the corrosion of copper to acceptable levels. These figures reveal that rate of copper corrosion in a 2.0 mol·dm^{-3} H_2SO_4 solution in the presence of inhibitors were reduced with an increase in the concentrations of PEG 400, PEG 4000, and PVP K15 solutions at all the temperatures studied. On comparing the inhibition of corrosion rates, it is seen that the corrosion rates of copper in a 2.0 mol·dm^{-3} H_2SO_4 solution have been retarded in the following order: PVP K15 > PEG 4000 > PEG 400 at various temperatures.

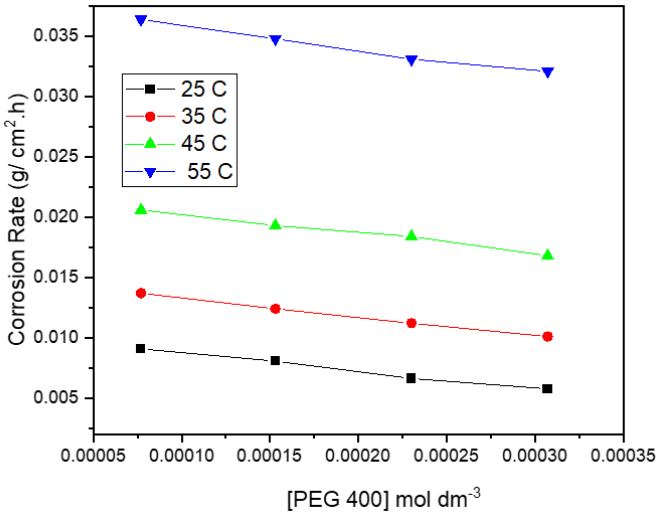

Figure 2. The corrosion rate of copper against various [PEG 400] in a 2.0 mol·dm^{-3} H_2SO_4 solution at different temperatures.

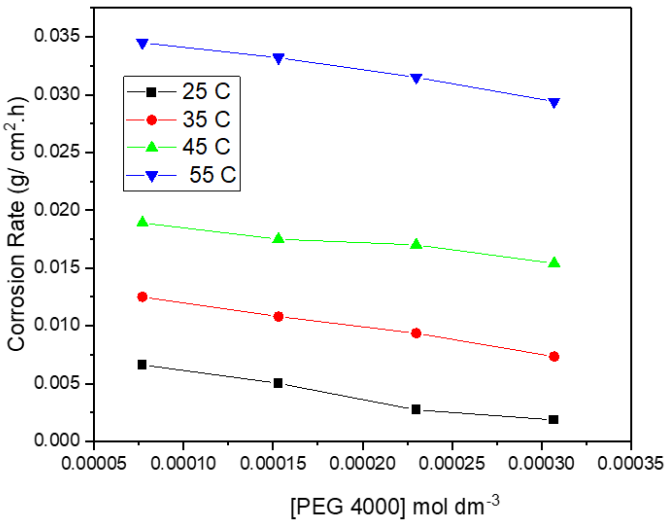

Figure 3. The corrosion rate of copper against various [PEG 4000] in a 2.0 mol dm^{-3} H_2SO_4 solution at different temperatures.

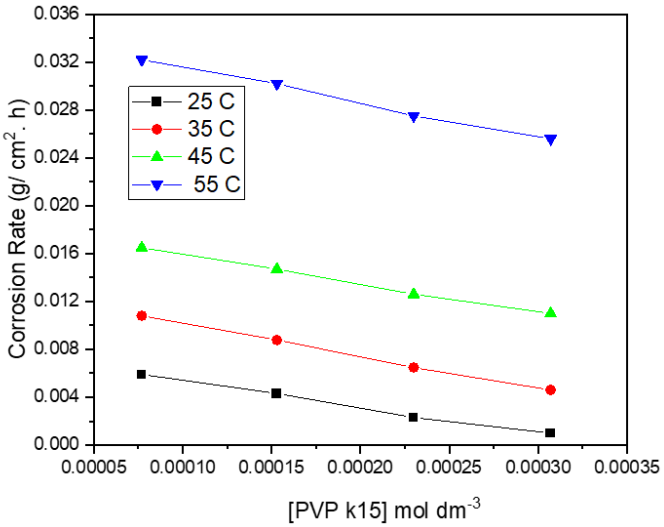

Figure 4. The corrosion rate of copper against various [PVP K15] in a 2.0 mol·dm^{-3} H_2SO_4 solution at different temperatures.

Tables 1–3 show the inhibition efficiencies of the inhibitors versus their concentrations at 25–55°C. However, these tables disclose that the inhibition efficiency of PVP K15 is higher than that of PEG 400 and PEG 4000 at all temperatures. While the inhibition efficiency of PEG 4000 is somewhat better than that of PEG 400, on the other hand, in all cases, the inhibition efficiencies decrease with an increase in temperature. For example, the inhibition efficiency of $3.07 \cdot 10^{-4}$ mol·dm^{-3} of PVP K15 exceeded 89% at 25°C, but this value decreased to reach 31% at 55°C. Thus, the superior inhibition efficiency of PVP K15 can be attributed to the presence of the π-system as well as O and N as heteroatoms inside very long PVP K15 chains, which play an important role in the interaction of π electrons and uncharged electron pairs in the chains with the copper surface *via* the adsorption process, resulting in an increase in the degree of surface coverage (θ) [25–30, 31]. In turn, the inverse relationship between inhibition efficiency and increasing temperatures indicate the mechanism of adsorption is physical adsorption.

Table 1. Change of the inhibition efficiency of PEG 400 at different concentrations for copper corrosion in a 2.0 mol·dm^{-3} H_2SO_4 solution for a 15.0-hour immersion period at different temperatures (25–55°C).

Concentration of PEG 400	**Inhibition efficiency (%I) at 25°C**	**Inhibition efficiency (%I) at 35°C**	**Inhibition efficiency (%I) at 45°C**	**Inhibition efficiency (%I) at 55°C**
0.000077 M	7.26	3.52	3.29	2.21
0.000153 M	21.59	12.68	9.39	6.70
0.00023 M	32.31	21.13	13.50	11.26
0.000307 M	41.10	28.88	17.06	14.21

Table 2. Change of the inhibition efficiency of PEG 4000 at different concentrations for copper corrosion in a 2.0 mol·dm^{-3} H_2SO_4 solution for a 15.0-hour immersion period at different temperatures (25–55°C).

Concentration of PEG 4000	Inhibition efficiency (%I) at 25°C	Inhibition efficiency (%I) at 35°C	Inhibition efficiency (%I) at 45°C	Inhibition efficiency (%I) at 55°C
0.000077 M	32.30	11.97	11.26	7.08
0.000153 M	53.57	23.94	17.84	11.00
0.00023 M	70.09	34.08	21.18	15.55
0.000307 M	80.87	41.09	25.1	17.19

Table 3. Change of the inhibition efficiency of PVP K15 at different concentrations for copper corrosion in a 2.0 mol·dm^{-3} H_2SO_4 solution for a 15.0-hour immersion period at different temperatures (25–55°C).

Concentration of PVP K15	Inhibition efficiency (%I) at 25°C	Inhibition efficiency (%I) at 35°C	Inhibition efficiency (%I) at 45°C	Inhibition efficiency (%I) at 55°C
0.000077 M	39.67	23.9	22.54	13.67
0.000153 M	59.83	41.17	31.99	22.04
0.00023 M	74.48	54.37	41.85	26.27
0.000307 M	89.78	67.54	48.36	31.37

3.3. Thermodynamic adsorption parameters

The performance of a chemical compound as an effective corrosion inhibitor depends on its capability to be adsorbed on the surface metal at various temperatures, which leads to the replacement of corrosive molecules at a corrodible interface. Therefore, the adsorption process of these organic or inorganic molecules on the metal surface is influenced by their electronic structures, in addition to the steric factors, aromaticity, and electronic density at the donor atoms [28–32]. In general, thermodynamic adsorption in the corrosion inhibition process is divided into physical and chemical adsorption. Physical adsorption is the electrostatic interaction between the ionic charges or dipoles of the inhibitor molecules and the electric charge at the surface of a metal. As a result, because the heat of physical adsorption is nearly zero, it will be stable at low temperatures. On the other hand, chemical adsorption takes place by charge sharing or transfer from the molecules of inhibitors to the metal surface to construct new chemical bonds. These formed bonds are stronger and more stable at higher temperatures compared with physical adsorption [33, 34].

The data obtained from the current work showed that the inhibition efficiencies of PEG 400, PEG 4000, and PVP K15 were enhanced with an increase in the concentration of the inhibitors, while they were reduced with an increase in temperature. The inhibition of copper corrosion by PEG 400, PEG 4000, and PVP K15 can be attributed to the physical

adsorption of inhibitor molecules on the surface of copper, whereas the decrease in inhibition efficiency with an increase in temperature is a result of the desorption process of the inhibitor molecules from the copper surface at higher temperatures [35, 36]. Because of the presence of π-systems in addition to oxygen and nitrogen atoms with lone pairs of electrons, which promote easy electron exchange with copper atoms (which have vacant d orbitals) on the copper surface, these complexes will cover a large surface area as an adhesive layer to protect the copper from the corrosive agents present in the solution [37, 38]. Undoubtedly, the molecular weight of the polymer as a corrosion inhibitor plays an important role in the interactions between inhibitor molecules and the metal surface; this is evident by the high inhibition efficiency of PEG 4000 in comparison with PEG 400.

Figures 5–7 depict the Temkin adsorption isotherm relationship between the number of PEG 400, PEG 4000, and PVP K15 molecules adsorbed on a unit area of the copper surface as a function of the logarithm of the inhibitor concentration in corrosive solutions at different temperatures. The values of surface coverage (θ) for various concentrations of the inhibitors were studied at 25–55°C by Temkin equation (4) to interpret the best isotherm model to determine the suitable adsorption process during the corrosion inhibition mechanism. Where *a* is the molecular interaction parameter in the adsorption layer and the heterogeneity of the metal surface, θ is the degree of surface coverage, *K* is the equilibrium constant of the adsorption process, and *C* is the concentration of the inhibitors. Accordingly, the linear relationship between θ and the logarithm of the concentrations of PEG 400, PEG 4000, and PVP K15 indicates that they obey the Temkin adsorption isotherm at the temperatures studied [29, 30].

$$\exp(-2a\theta) = KC \tag{4}$$

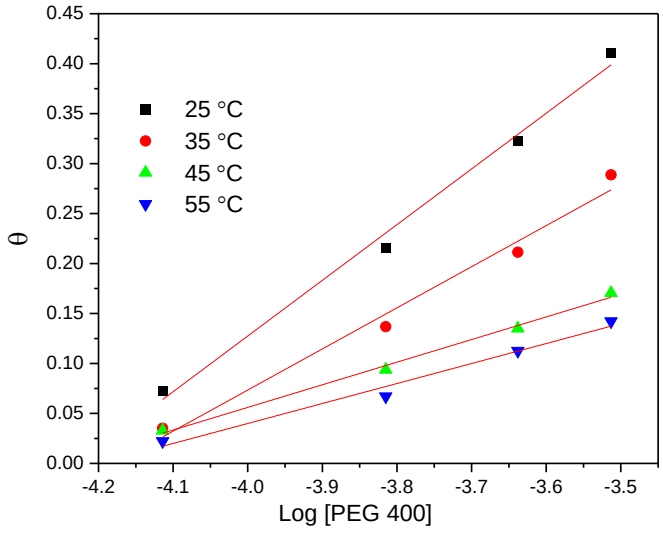

Figure 5. Temkin adsorption isotherm plot for the inhibitor PEG 400 at different temperatures (Surface coverage (θ) *versus* Log inhibitor concentration).

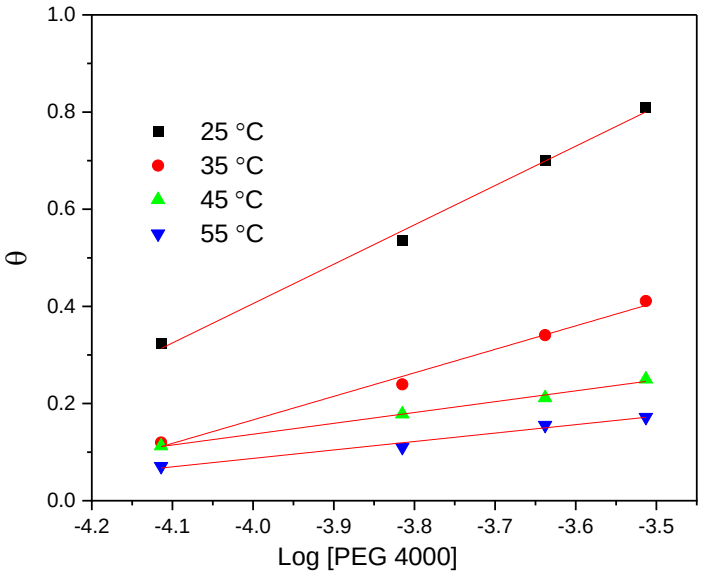

Figure 6. Temkin adsorption isotherm plot for the inhibitor PEG 4000 at different temperatures (Surface coverage (θ) *versus* Log inhibitor concentration).

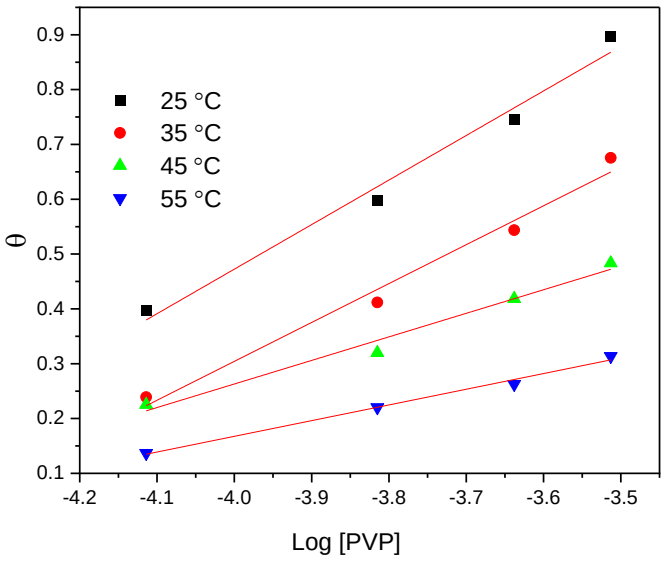

Figure 7. Temkin adsorption isotherm plot for the inhibitor PVP K15 at different temperatures (Surface coverage (θ) *versus* Log inhibitor concentration).

Table 4 exhibits the values of that calculated by the Temkin equation, which is smaller than zero at all temperatures, referring to the repulsion that exists in the adsorption layer [39]. Here, the linear correlation coefficients are perfect in all experiments. *K* value denotes the strength of the interaction between inhibitor molecules and the metal surface in the same

context. Hence, larger values of *K* point to efficient adsorption and hence better inhibition efficiency. Furthermore, the values of *K* presented in Table 4 illustrate that the adsorption coefficients decline as the temperature rises. Nonetheless, *K* values for PVP K15 are higher than PEG 400 and PEG 4000 to reflect the significant ability of PVP K15 molecules to adsorb on the copper surface due to the presence of characteristic heteroatoms and π-bonds inside long polymer chains.

Table 4. Parameters of the linear regression from Temkin isotherm plot.

Inhibitor	Temperature (°C)	A	K (M^{-1})	Linear correlation coefficient
PEG 400	25	–0.68	226.98	0.993
	35	–0.71	52.36	0.985
	45	–0.67	9.12	0.995
	55	–0.70	6.90	0.982
PEG 4000	25	–0.50	4365.16	0.995
	35	–0.58	125.89	0.991
	45	–0.44	10.72	0.994
	55	–0.50	6.03	0.984
PVP K15	25	–0.45	5248.07	0.983
	35	–0.52	1380.38	0.983
	45	–0.43	91.20	0.991
	55	–0.45	20.42	0.992

In turn, the plot of $\log[\theta/(1-\theta)]$ *versus* $\log C$ was investigated for its appropriateness to the Langmuir adsorption isotherm model, which is elucidated by equation (5): where θ is the surface coverage degree, *K* represents the equilibrium constant for the adsorption process, and *C* is the inhibitor concentration. Anyway, linear plots were achieved, as shown in Figures 8–10, which indicates that the experimental data obey the Langmuir adsorption isotherm at all temperatures. The application of Flory–Huggins' isotherm model to the adsorption of inhibitors on the surface of copper, on the other hand, is illustrated by equation (6) [40–42]. Unfortunately, these green inhibitors disobeyed the Flory–Huggins adsorption isotherm, as seen in Figure 11.

$$\frac{\theta}{1-\theta} = KC \tag{5}$$

$$KC = \left[\frac{\theta}{(1-\theta)^x}\right]\exp(1-x) \tag{7}$$

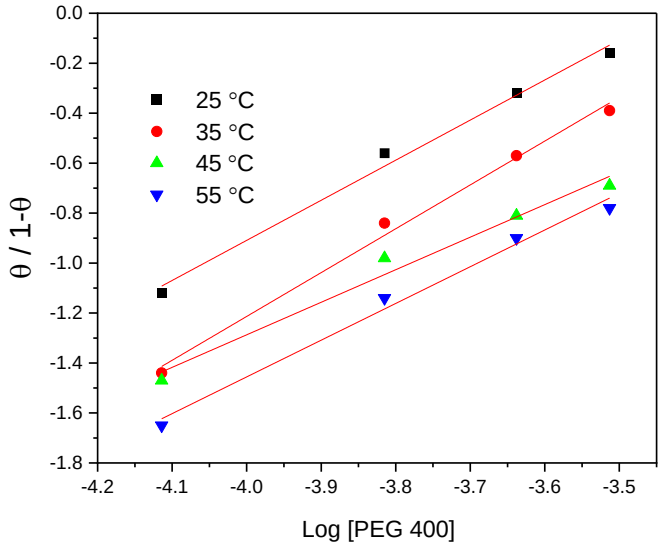

Figure 8. Langmuir adsorption isotherm plot for the inhibitor PEG 400 at different temperatures (Log Surface coverage (θ)/(1–θ) *versus* Log inhibitor concentration).

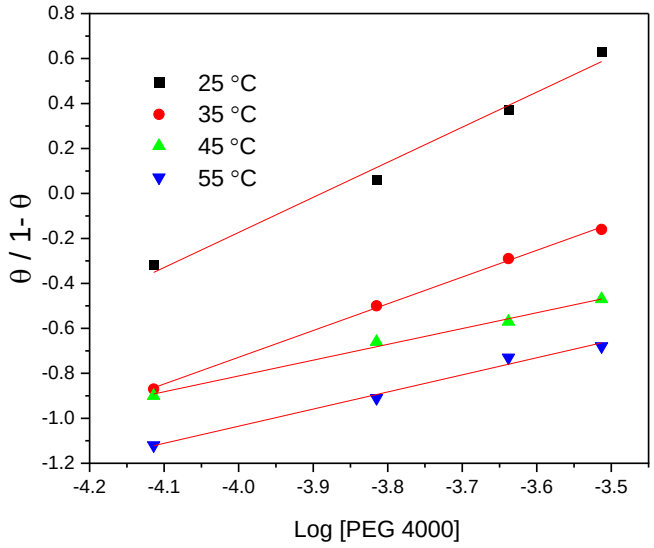

Figure 9. Langmuir adsorption isotherm plot for the inhibitor PEG 4000 at different temperatures (Log Surface coverage (θ)/(1–θ) *versus* Log inhibitor concentration).

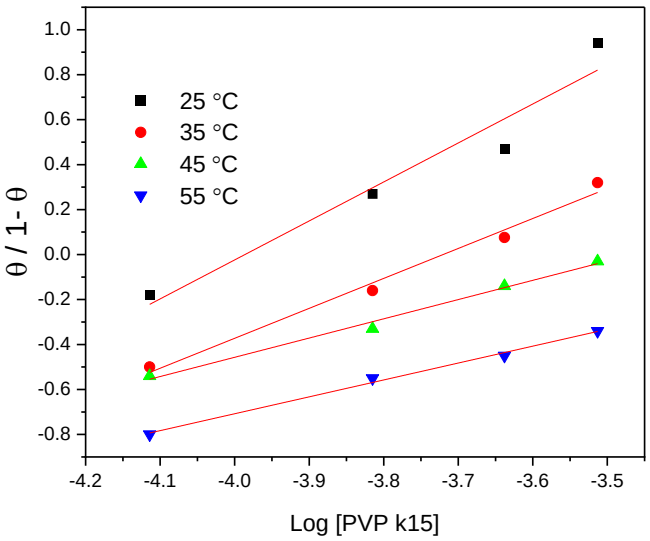

Figure 10. Langmuir adsorption isotherm plot for the inhibitor PVP K15 at different temperatures (Log Surface coverage (θ)/(1–θ) *versus* Log inhibitor concentration).

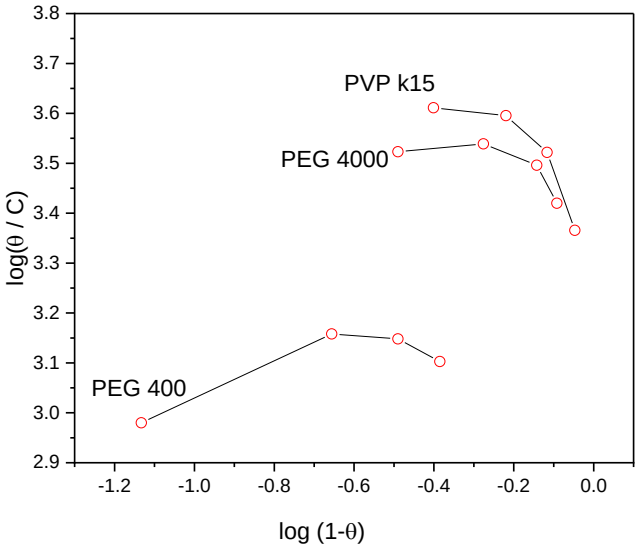

Figure 11. Flory–Huggins adsorption isotherm plot for the inhibitors PEG 400, PEG 4000, and PVP K15 with a copper surface in a 2.0 mol·dm^{-3} H_2SO_4 solution at 25°C.

3.4. Thermodynamic studies

The influence of temperature on copper corrosion in a 2.0 mol·dm^{-3} H_2SO_4 solution in the absence and presence of PEG 400, PEG 4000, and PVP K15 was explored from 25 to 55°C. The thermodynamic results obtained in the current work displayed that an increase in temperature leads to an increase in the corrosion rate as well as a decrease in inhibition efficiency at all concentrations of inhibitors. In this regard, the activation energy (E_a) of copper corrosion in a 2.0 mol·dm^{-3} H_2SO_4 solution in the absence and presence of PEG 400, PEG 4000, and PVP K15 was evaluated by the Arrhenius equation (7):

$$\log CR = \log A - \frac{E_a}{2.303RT}, \quad (7)$$

where CR is the rate of corrosion, A is the Arrhenius constant, R is the molar gas constant, and T is the absolute temperature.

Table 5. Activation parameters for copper corrosion in the presence of PEG 400, PEG 4000, and PVP K15 in a 2.0 mol·dm^{-3} H_2SO_4 solution.

Inhibitor / Concentration	E_a (kJ/mol)	$\Delta H^{\#}$ (kJ/mol)	$\Delta S^{\#}$ (J/mol·K)
Blank	35.25	14.66	
	PEG 400		
0.000077	37.18	15.32	–183.91
0.000153	41.20	16.73	–179.74
0.00023	43.67	17.65	–177.08
0.000307	47.1	19.05	–172.93
	PEG 4000		
0.000077	44.22	17.79	–176.50
0.000153	52.78	21.85	–164.11
0.00023	65.22	27.84	–154.82
0.000307	75.71	32.41	–131.86
	PVP K15		
0.000077	45.5	18.45	–174.84
0.000153	53.91	22.33	–163.20
0.00023	66.61	27.61	–147.24
0.000307	87.40	37.41	–117.39

Plotting $\log CR$ *versus* $1/T$ yields straight lines, as shown in Figures 12–14. The values of E_a were estimated from the slope of straight lines, as illustrated in Table 5. The E_a values were discovered to increase in the following order as inhibitor concentrations increased: PVP K15 > PEG 4000 > PEG 400 at different temperatures compared to the blank, and consequently, the rates of copper corrosion were retarded. The enthalpy and entropy of activation of copper dissolution in a 2.0 mol·dm^{-3} H_2SO_4 solution were also calculated *via* the following transition state equation (8):

$$CR = \frac{RT}{Nh}\exp\left(\frac{\Delta S^{\#}}{RT}\right)\exp\left(\frac{-\Delta H^{\#}}{RT}\right), \quad (8)$$

where h is Planck's constant and N is Avogadro's number. The plots of $\ln(CR/T)$ against $1/T$ are displayed in Figures 12–14, which show a straight line with slope and intercept, are $-\Delta H^{\#}/R$ and $\ln(R/Nh) + (\Delta S^{\#}/R)$, respectively. The values of entropy ($\Delta S^{\#}$) and enthalpy ($\Delta H^{\#}$) as elucidated in Table 5 indicate that the activation complex in the rate-determining step during the corrosion process represents association rather than dissociation, resulting in a reduction in randomness on the way from the reactants to the activated complex.

While, the free energy of adsorption, ΔG^{0}_{ads} values obtained using the following equation (9):

$$K = \frac{1}{55.5}\exp\left(\frac{-\Delta G^{0}_{ads}}{RT}\right) \tag{9}$$

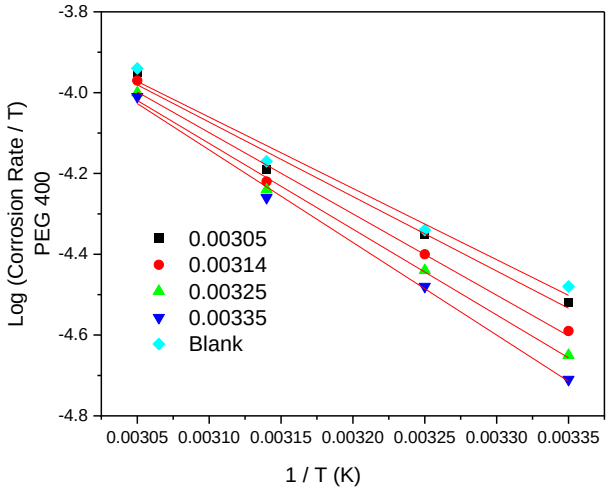

Figure 12. Transition state plot as log (CR/T) *versus* $1/T$ for copper in a 2.0 mol·dm^{-3} H_2SO_4 solution containing different concentrations of PEG 400.

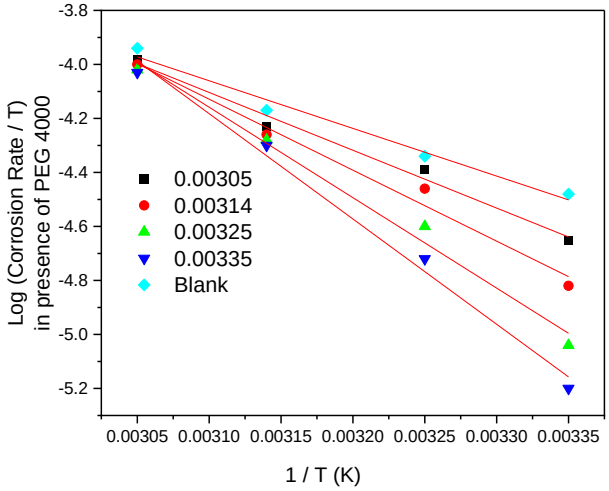

Figure 13. Transition state plot as log(CR/T) *versus* $1/T$ for copper in a 2.0 mol·dm^{-3} H_2SO_4 solution containing different concentrations of PEG 4000.

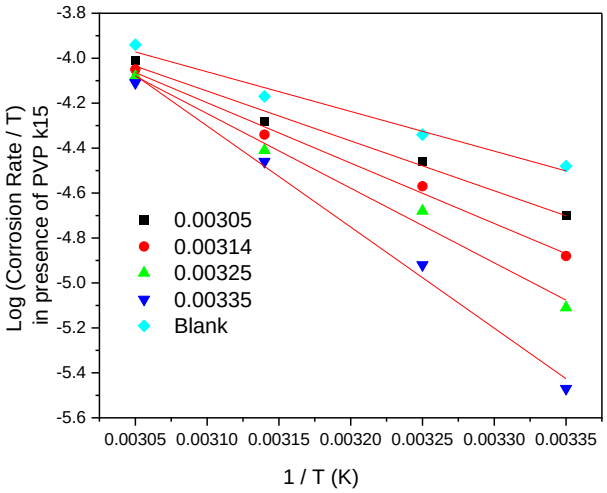

Figure 14. Transition state plot as $\log(CR/T)$ *versus* $1/T$ for copper in a 2.0 mol·dm^{-3} H_2SO_4 solution containing different concentrations of PVP K15.

The value of 55.5 is the concentration of water in the solution expressed in mol, while K is the equilibrium constant of the adsorption process. The free energies of adsorption ΔG^0_{ads} have been calculated from equation (8) for the inhibitors PEG 400, PEG 4000, and PVP K15. Table 6 shows ΔG^0_{ads} values for all inhibitors at (25–55°C) to reveal that ΔG^0_{ads} values for PEG 400 ranged from –7.05 kJ/mol to –10.16 kJ/mol with an average value of –8.31 kJ/mol. The ΔG^0_{ads} values for PEG 4000 are 6.89 kJ/mol to –13.12 kJ/mol with an average of –9.30 kJ/mol. In turn, the ΔG^0_{ads} values for PVP K15 range from –8.36 kJ/mol to –13.31 kJ/mol, with an average of –11.00 kJ/mol. As a result, the values of ΔG^0_{ads} indicate that the inhibitor molecules spontaneously adsorb to the copper surface. Remarkably, the average ΔG^0_{ads} value for PVP K15 is relatively more negative than that for PEG 400 and PEG 4000, which indicates the high adsorption efficiency of PVP K15 with copper atoms at various concentrations and temperatures. ΔG^0_{ads} values less than –40 kJ/mol, on the other hand, are consistent with the nature of the electrostatic interaction between the inhibitor molecules and the copper surface *via* weak physical adsorption [43–46]. On the other hand, by employing equation (10) to plot ΔG^0_{ads} against T as shown in Figures 15–17, the entropy of adsorption (ΔS^0_{ads}) and enthalpy of adsorption (ΔH^0_{ads}) was estimated by the slope and the intercept, respectively. The obtained values of the line parameters are listed in Table 6. In this regard, the negative values of ΔH^0_{ads} refer to the adsorption of inhibitor molecules on copper surfaces, which follows exothermic physical adsorption. Furthermore, the negative ΔS^0_{ads} values in a 2.0 mol·dm^{-3} H_2SO_4 solution indicate a decrease in randomness moving from reactants to adsorbed species.

$$\Delta G^0_{ads} = \Delta H^0_{ads} - T\Delta S^0_{ads} \quad (10)$$

Table 6. Thermodynamic parameters for the adsorption of the inhibitors during copper corrosion at different temperatures.

Inhibitor	Temperature (°C)	K (M^{-1})	ΔH^0 (kJ/mol)	ΔS^0 (J/mol·K)	ΔG^0_{ads} (kJ/mol)	Linear correlation coefficient
PEG 400	25	226.98	–48.84	–130.04	–10.16	0.993
	35	52.36			–8.87	0.985
	45	9.12			–6.69	0.995
	55	6.90			–6.40	0.982
PEG 4000	25	4365.16	–89.56	–258.1	–13.33	0.995
	35	125.89			–9.52	0.991
	45	10.72			–6.87	0.994
	55	6.00			–6.25	0.984
PVP K15	25	5248.07	–77.76	–208.2	–13.54	0.983
	35	1380.38			–12.09	0.983
	45	91.20			–9.18	0.991
	55	20.42			–7.57	0.992

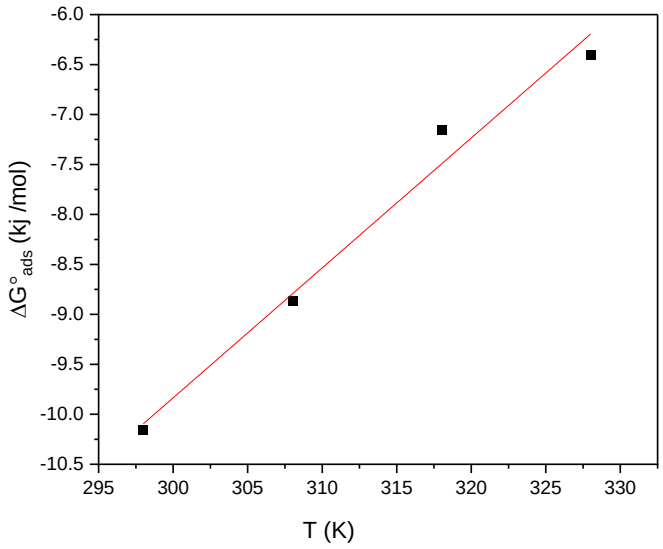

Figure 15. Plot of ΔG^0_{ads} *versus T* for the adsorption of PEG 400 in a 2.0 mol·dm^{-3} H_2SO_4 solution.

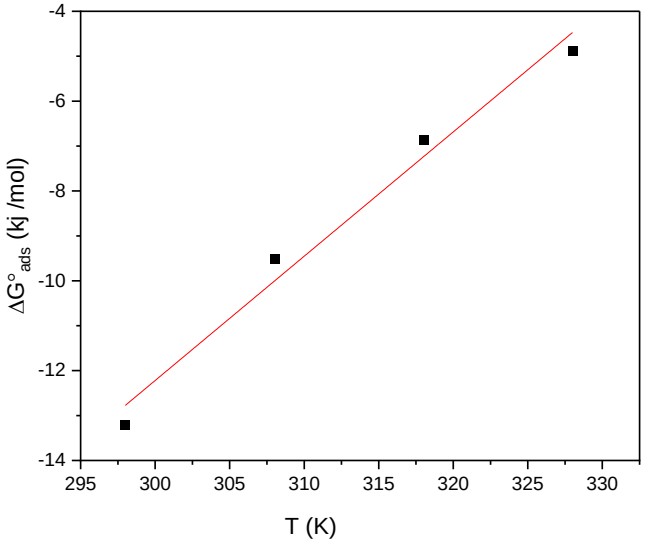

Figure 16. Plot of ΔG^0_{ads} *versus T* for the adsorption of PEG 4000 in a 2.0 mol·dm^{-3} H_2SO_4 solution.

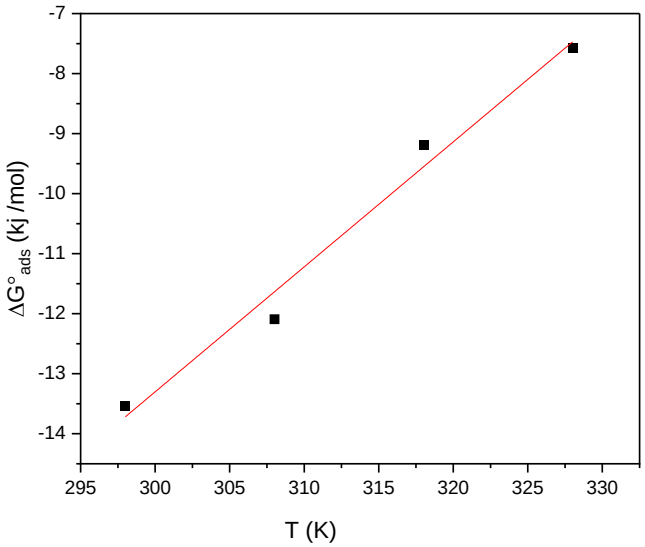

Figure 17. Plot of ΔG^0_{ads} *versus T* for the adsorption of PVP K15 in a 2.0 mol·dm^{-3} H_2SO_4 solution.

3.5. Electrical conductance measurements and mechanism of the copper corrosion

Copper corrosion rates in aerated H_2SO_4 solutions depend considerably on the length of time of contact between the copper surface and the corrosive environment [47]. When copper is immersed in a 2.0 mol·dm^{-3} H_2SO_4 solution in the presence of atmospheric oxygen as a powerful oxidising agent in the corrosive medium, copper will start to corrode, giving off Cu^{2+} ions, and then the accumulated Cu^{2+} ions in the solution will react with metallic copper

to release Cu^{+} ions, which will be reoxidised by oxygen to provide further Cu^{2+} ions according to the following chemical reactions [48, 49]:

$$2Cu + O_2 + 2H_2SO_4 \rightarrow 2CuSO_4 + 2H_2O$$

$$Cu^{+2}_{(aq)} + Cu_{(s)} \rightarrow 2Cu^{+}_{(aq)}$$

Figure 17 shows the change in the electrical conductance by time in a 2.0 mol·dm^{-3} H_2SO_4 solution in the presence and absence of 3.05×10^{-4} mol·dm^{-3} of PEG 400, PEG 4000, and PVP K15 at 25°C. The electrical conductance increases with time as the corrosion process progresses, increasing the concentration of Cu^{+2} ions in an acidic solution. Generally, the electrical conductance of solutions depends on the ionic charge, concentration, and mobility of the solute [50]. On the other hand, in the presence of inhibitors, the electrical conductance was reduced in the initial stage of electrical measurement compared to the blank solution, and then the electrical conductance became almost constant in the remaining time under the hindrance of generating further Cu^{+2} ions in the corrosive solution, which confirms a significant inhibition property of PEG 400, PEG 4000, and PVP K15 in the corrosion process.

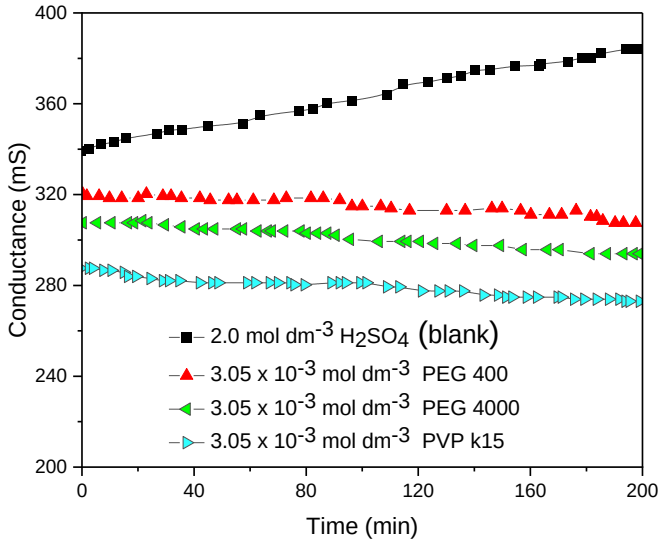

Figure 18. The changes in electrical conductance by time for copper specie immersed in a 2.0 mol·dm^{-3} H_2SO_4 solution in the presence and absence of 3.05×10^{-4} mol·dm^{-3} of PEG 400, PEG 4000, and PVP K15 at 25°C.

Conclusion

Polyethylene glycol 400, 4000, and polyvinylpyrrolidone K15 were investigated for their potential use as green inhibitors for copper corrosion in various concentrations of sulfuric acid solutions by using gravimetric, thermometric, and electrical conductance techniques. It was found that their inhibition efficiencies increased with an increase in the concentration

of the inhibitors. In all cases, the inhibition efficiency of PVP K15 was higher than that of PEG 400 and PEG 4000. Accordingly, the protective effect of these inhibitors might be attributed to the nature of functional groups, lengths of polymer chains, and their adsorption ability on the copper surface. On the other hand, PEG 400, PEG 4000, and PVP K15 were found to obey the Temkin and Langmuir adsorption isotherms at all temperatures studied. The thermodynamic adsorption free energy (ΔG^0_{ads}) value and sign indicate that the process was spontaneous and exothermic.

Acknowledgements

The authors would like to thank Philadelphia University and Al-Balqa Applied University in Jordan for successfully carrying out all experimental runs in their scientific laboratories.

References

1. M. Amini, M. Toorani and A.S. Rouhaghdam, Corrosion of Copper in 0.1 M Hydrochloric Acid Solution with Benzotriazole as Corrosion Inhibitor, *Prot. Met. Phys. Chem. Surf*., 2020, **56**, 803–815. doi: 10.1134/s2070205120040048
2. D.M. Bastidas, Adsorption of benzotriazole on copper surfaces in a hydrochloric acid solution, *Surf. Interface Anal*., 2006, **38**, 1146–1152. doi: 10.1002/sia.2371
3. C. Verma, E.E. Ebenso, M.A. Quraishi and C.M. Hussain, Recent developments in sustainable corrosion inhibitors: design, performance and industrial scale applications, *Mater. Adv*., 2021, **2**, 3806–3850. doi: 10.1039/d0ma00681e
4. E.M. Sherif, R.M. Erasmus and J.D. Comins, Corrosion of Copper in Aerated Acidic Pickling Solutions and Its Inhibition by 3-Amino-1,2,4-Triazole-5-Thiol, *J. Colloid Interface Sci*., 2007, **306**, 96–104. doi: 10.1016/j.jcis.2006.10.029
5. S.M.A. Hosseini and A. Azimi, The inhibition of mild steel corrosion in acidic medium by 1-methyl-3-pyridin-2-yl-thiourea, *Corros. Sci*., 2009, **51**, 728–732. doi: 10.1016/j.corsci.2008.11.019
6. P.C. Okafor and Y. Zheng, Synergistic inhibition behaviour of methylbenzyl quaternary imidazoline derivative and iodide ions on mild steel in H_2SO_4 solutions, *Corros. Sci*., 2009, **51**, 850–859. doi: 10.1016/j.corsci.2009.01.027
7. A.I. Muñoz, J.G. Antón, J.L. Guiñón and V.P. Herranz, Comparison of inorganic inhibitors of copper, nickel and copper–nickels in aqueous lithium bromide solution, *Electrochim. Acta*, 2004, **50**, 957–966. doi: 10.1016/j.electacta.2004.07.048
8. H. Gerengi, K. Darowick, P. Slepski, G. Bereket and J. Ryl, Investigation effect of benzotriazole on the corrosion of brass-MM55 alloy in artificial seawater by dynamic EIS, *J. Solid State Electrochem*., 2009, **14**, 897–902. doi: 10.1007/s10008-009-0923-1
9. W.J. Lee, Inhibiting effects of imidazole on copper corrosion in 1 M HNO_3 solution, *Mater. Sci. Eng*., 2003, **348**, 217–226. doi: 10.1016/s0921-5093(02)00734-7

10. M. Finšgar, 2-Mercaptobenzimidazole as a copper corrosion inhibitor: Part I. Long-term immersion, 3D-profilometry, and electrochemistry, *Corros. Sci*., 2013, **72**, 82–89. doi: 10.1016/j.corsci.2013.03.011
11. Y.M. Abdallah and K. Shalabi, Comprehensive study of the behavior of copper inhibition in 1 M HNO_3 by Euphorbia Helioscopia linn. extract as green inhibitor, *Prot. Met. Phys. Chem. Surf*., 2015, **51**, 275–284. doi: 10.1134/s2070205115020021
12. M. Amini, M. Toorani and A.S. Rouhaghdam, Corrosion of Copper in 0.1 M Hydrochloric Acid Solution with Benzotriazole as Corrosion Inhibitor, *Prot. Met. Phys. Chem. Surf*., 2020, **56**, 803–815. doi: 10.1134/s2070205120040048
13. R.S. Al-Moghrabi, A.M. Abdel-Gaber and H.T. Rahal, Corrosion Inhibition of Mild Steel in Hydrochloric and Nitric Acid Solutions Using Willow Leaf Extract, *Prot. Met. Phys. Chem. Surf*., 2019, **55**, 603–607. doi: 10.1134/s2070205119030031
14. A.M. Abdel-Gaber, H.T. Rahal and F.T. Beqai, Eucalyptus leaf extract as an eco-friendly corrosion inhibitor for mild steel in sulfuric and phosphoric acid solutions, *Int. J. Ind. Chem*., 2020, **11**, 123–132. doi: 10.1007/s40090-020-00207-z
15. L.W. El Khatib, H.T. Rahal and A.M. Abdel-Gaber, Synergistic Effect between *Fragaria ananassa* and *Cucurbita pepo L* Leaf Extracts on Mild Steel Corrosion in Hydrochloric Acid Solutions, *Prot. Met. Phys. Chem. Surf*., 2020, **56**, no. 5, 1096–1106. doi: 10.1134/s2070205120050111
16. K.M. Hijazi, A.M. Abdel-Gaber, G.O. Younes and R. Habchi, Comparative study of the effect of an acidic anion on the mild steel corrosion inhibition using *Rhus Coriaria* plant extract and its quercetin component, *Port. Electrochim. Acta*, 2021, **39**, 237–252. doi: 10.4152/pea.2021390402
17. R. Kardooni and A.R. Kiasat, Polyethylene Glycol (PEG-400): A Green Reaction Medium for One-Pot, Three Component Synthesis of 3-Substituted Indoles under Catalyst Free Conditions, *Polycyclic Aromat. Compd*., 2019, 1–9. doi: 10.1080/10406638.2019.1703764
18. A. Dahadha, M. Hassan, M. Al-Dhoun, Y. Batineh and M. Abu-Halaweh, Kinetics of oxidation of aspirin by Ce(IV) in surfactant, polymer, and mixed surfactant-polymer media, *Colloid Polym. Sci*., 2021, **299**, 1315–1326. doi: 10.1007/s00396-021-04849-y
19. M. Hassan, M. Al-Dhoun, Y. Batineh, A.A. Najjar, A. Dahadha and Q.A. Ibrahim, Micellar and polymer catalysis in the kinetics of oxidation of L-lysine by permanganate ion in perchloric acid medium, *S. Afr. J. Chem*., 2021, **75**, 73–79. doi: 10.17159/0379-4350/2021/v75a8
20. A.A. Dahadha, M.J. Saadh, T. Mfarej, M. Hassan, M. Abunuwar and N.T. Talat, Polyethylene glycols catalyzed reaction of catechol and resorcinol with cerium ammonium sulfate in the aqueous medium: kinetic and mechanistic study, *Chem. Afr*., 2022, **5**, 1417–1426. doi: 10.1007/s42250-022-00436-y

21. A.A. Dahadha, M. Hassan, T. Mfarej, R. Bani Issa, M.J. Saadh, M. Al-Dhoun, M. Abunuwar and N.T. Talat, The Catalytic Influence of Polymers and Surfactants on the Rate Constants of Reaction of Maltose with Cerium(IV) in Acidic Aqueous Medium, *J. Chem*., 2022, 2609478. doi: 10.1155/2022/2609478
22. A.A. Dahadha, M. Hassan, T. Mfarej, M. Al-Dhoun, M. Abunuwar and Y. Batineh, The effect of mixed sodium dodecyl sulfate – polyethylene glycol systems on kinetic of oxidation of *o*-Cresol by cerium(IV) in H_2SO_4 medium, *Colloid Polym. Sci*., 2022, **300**, 177–190. doi: 10.1007/s00396-022-04940-y
23. A.A. Dahadha, M. Hassan, M. Al-Dhoun, T. Mfarej, M. Abunuwar and Y. Batineh, The oxidation of salicylic acid and acetylsalicylic acid by water soluble colloidal manganese oxide in surfactant and polymer media: a kinetic and mechanistic approach, *React. Kinet., Mech. Catal*., 2021, **134**, 37–55. doi: 10.1007/s11144-021-02083-9
24. H.A. Sorkhabi and N.G. Jeddi, Inhibition effect of polyethylene glycol on the corrosion of carbon steel in sulphuric acid, *Mater. Chem. Phys*., 2005, **92**, 480–486. doi: 10.1016/j.matchemphys.2005.01.059
25. R. Vani, B.M. Praveen and G. Kuma, Polyethylene Glycol as a Corrosion Inhibitor for Lead and Lead Free Solders in Acidic Medium, *Int. J. Mech. Eng. & Rob Res*., 2015, **4**, 128–135.
26. S. Salimi, M. Nasr-Esfahani, S.A. Umoren and E. Saebnoori, Complexes of Imidazole with Poly(ethylene glycol) as a Corrosion Inhibitor for Carbon Steel in Sulphuric Acid, *J. Mater. Eng. Perform*., 2015, **24**, 4696–4709. doi: 10.1007/s11665-015-1788-3
27. L.A. Al Juhaiman, A. Abu Mustafa and W.K. Mekhame, Polyvinyl Pyrrolidone as a Green Corrosion Inhibitor of Carbon Steel in Neutral Solutions Containing NaCl: Electrochemical and Thermodynamic Study, *Int. J. Electrochem. Sci*., 2012, **7**, 8578–8596.
28. L.A. Al Juhaiman, Polyvinyl pyrrolidone as a Corrosion Inhibitor for Carbon Steel in HCl, *Int. J. Electrochem. Sci*., 2016, **11**, 2247–2262.
29. S.A. Umoren, O. Ogbobe, P.C. Okafor and E.E. Ebenso, Polyethylene glycol and polyvinyl alcohol as corrosion inhibitors for aluminium in acidic medium, *J. Appl. Polym. Sci*., 2007, **105**, 3363–3370. doi: 10.1002/app.26530
30. S.A. Umoren, E.E. Ebenso, P.C. Okafor and O. Ogbobe, Water-soluble polymers as corrosion inhibitors, *Pigm. Resin Technol*., 2006, **35**, 346–352. doi: 10.1108/03699420610711353
31. F. Bentiss, M. Lagrenee, M. Traisnel and J.C. Hornez, The corrosion inhibition of mild steel in acidic media by a new triazole derivative, *Corros. Sci*., 1999, **41**, 789–803. doi: 10.1016/S0010-938X(98)00153-X
32. E. McCafferty, V. Pravdic and A.C. Zettlemoyer, Dielectric behaviour of adsorbed water films on the α-Fe_2O_3 surface, *Trans. Faraday Soc*., 1970, **66**, 1720–1731.

33. F. Bentiss, M. Lebrini and M. Lagrenee, Thermodynamic characterization of metal dissolution and inhibitor adsorption processes in mild steel/2,5-bis(*n*-thienyl)-1,3,4-thiadiazoles/hydrochloric acid system, *Corros. Sci*., 2005, **47**, 2915–2931. doi: 10.1016/j.corsci.2005.05.034
34. P.M. Niamien, H.A. Kouassi, A. Trokourey, F.K. Essy, D. Sissouma and Y. Bokra, Copper Corrosion Inhibition in 1 M HNO_3 by Two Benzimidazole Derivatives, *ISRN Mater. Sci*., 2012, 623754, 1–15. doi: 10.5402/2012/623754
35. M.A. Quraishi and H.K. Sharma, Thiazoles as corrosion inhibitors for mild steel in formic and acetic acid solutions, *J. Appl. Electrochem*., 2005, **35**, 33–39. doi: 10.1007/s10800-004-2055-8
36. M. Ajmal, D. Jamal and M.A. Quraishi, Fatty acid oxadiazoles as acid corrosion inhibitors for mild steel, *Anti-Corros. Methods Mater*., 2000, **47**, 77–82. doi: 10.1108/00035590010316412
37. P.C. Okafor and Y. Zheng, Synergistic inhibition behaviour of methylbenzyl quaternary imidazoline derivative and iodide ions on mild steel in H_2SO_4 solutions, *Corros. Sci*., 2009, **51**, 850–859. doi: 10.1016/j.corsci.2009.01.027
38. A.S. Fouda and A.S. Ellithy, Inhibition effect of 4-phenylthiazole derivatives on corrosion of 304L stainless steel in HCl solution, *Corros. Sci*., 2009, **51**, 868–875. doi: 10.1016/j.corsci.2009.01.011
39. L. Tang, X. Li, Y, Si, G. Mu and G. Liu, The synergistic inhibition between 8-hydroxyquinoline and chloride ion for the corrosion of cold rolled steel in 0.5M sulfuric acid, *Mater. Chem. Phys*., 2006, **95**, 29–38. doi: 10.1016/j.matchemphys.2005.03.064
40. H.T. Rahal, A.M. Abdel-Gaber and G.O. Younes, Inhibition of Steel Corrosion in Nitric Acid by Sulfur Containing Compounds, *Chem. Eng. Commun*., 2015, **203**, no. 4, 435–445. doi: 10.1080/00986445.2015.1017636
41. A.M. Abdel-Gaber, H.T. Rahal, M.S. El-Rifai, Green Approach towards Corrosion Inhibition in Hydrochloric Acid Solutions, *Biointerface Res. Appl. Chem*., 2021, **11**, 14185–14195.
42. M. Kilo, H.T. Rahal, M.H. El-Dakdouki and A.M. Abdel-Gaber, Study of the corrosion and inhibition mechanism for carbon steel and zinc alloys by an eco-friendly inhibitor in acidic solution, *Chem. Eng. Commun*., 2021, **208**, no. 12, 1676–1685. doi: 10.1080/00986445.2020.1811239
43. S. Bilgic and M. Sahin, The corrosion inhibition of austenitic chromium-nickel steel in H_2SO_4 by 2-butyn-1-ol, *Mater. Chem. Phys*., 2001, **70**, 290–295. doi: 10.1016/S0254-0584(00)00534-4
44. P.C. Okafor, E.E. Ebenso, U.J. Ekpe, U.J. Ibok and M.I. Ikpi, Inhibition of 4-acetamidoaniline on corrosion of mild steel in HCl solution, *Trans. SAEST*., 2003, **38**, 91–96
45. M.A. Al-Qudah, H.G. AL-Keifi, I.F. Al-Momani and S.T. Abu-Orabi, *Capparis Aegyptia* as a green inhibitor for aluminum corrosion in alkaline media, *Int. J. Corros. Scale Inhib*., 2020, **9**, 201–218. doi: 10.17675/2305-6894-2020-9-1-12

46. H. Al-sharabi, K. Bouiti, F. Bouhlal, N. Labjar, G. Amine Benabdellah, A. Dahrouch, L. Hermouch, S. Kaya, B. El Ibrahimi, M. El Mahi, E.M. Lotfi, B. El Otmani and S. El Hajjaji, Anti-corrosive properties of *Catha Edulis* leaves extract on C38 steel in 1 M HCl media. Experimental and theoretical study, *Int. J. Corros. Scale Inhib*., 2022, **11**, 956–984. doi: 10.17675/2305-6894-2022-11-3-4
47. Ya.G. Avdeev, K.L. Anfilov, E.P. Rukhlenko and Yu.I. Kuznetsov, Inhibitory protection of copper in acetic acid solutions, *Int. J. Corros. Scale Inhib*., 2021, **10**, no. 1, 302–313. doi: 10.17675/2305-6894-2020-10-1-17
48. Ya.G. Avdeev, K.L. Anfilov, E.P. Rukhlenko and Yu.I. Kuznetsov, Inhibitor protection of copper in citric acid solutions, *Int. J. Corros. Scale Inhib*., 2021, **10**, no. 3, 911–923. doi: 10.17675/2305-6894-2021-10-3-5
49. A. Sulcius, E. Griskonis and N. Zmuidzinaviciene, Copper Dissoliution in Concentrated Sulfuric Acid, *World J. Chem. Educ*., 2019, **7**, 196–202. doi: 10.12691/wjce-7-3-2
50. K.J. Laidler, J.H. Moiser and B.C. Sanctuary, *Physical chemistry*, Houghton Mifflin, Boston, 2003, p. 291.

♦ ♦ ♦

Supplementary Materials

Table 1S. Copper samples immersed in different concentrations of H_2SO_4 solution at 25°C for 15.0 hours.

Weight of copper piece (g)	Weight after immersed in H_2SO_4 (g)	Δ*w* (mg)	Corrosion rate g/cm^2·h	Concentration of H_2SO_4	Dimension (cm)
5.7578	5.7510	6.8	0.00978	2.0 mol·dm^{-3}	2.3×1.2×0.1
5.7037	5.6987	5.0	0.00720	1.5 mol·dm^{-3}	2.3×1.2×0.1
5.7024	5.6983	4.1	0.00590	1.0 mol·dm^{-3}	2.3×1.2×0.1
5.6916	5.6881	3.5	0.00502	0.5 mol·dm^{-3}	2.3×1.2×0.1

Table 2S. Copper samples immersed in different concentrations of H_2SO_4 solution at 35°C for 15.0 hours.

Weight of copper piece (g)	Weight after immersed in H_2SO_4 (g)	Δ*w* (mg)	Corrosion rate g/cm^2·h	Concentration of H_2SO_4 solution	Dimension (cm)
5.6765	5.6666	9.9	0.0142	2.0 mol·dm^{-3}	2.3×1.2×0.1
5.6689	5.6689	7.9	0.0108	1.5 mol·dm^{-3}	2.3×1.2×0.1
5.6659	5.6594	6.5	0.00936	1.0 mol·dm^{-3}	2.3×1.2×0.1
5.6639	5.6588	5.1	0.00733	0.5 mol·dm^{-3}	2.3×1.2×0.1

Table 3S. Copper samples immersed in different concentrations of H_2SO_4 solution at 45°C for 15.0 hours.

Weight of copper piece (g)	Weight after immersed in H_2SO_4 (g)	Δ*w* (mg)	Corrosion rate g/cm^2·h	Concentration of H_2SO_4 solution	Dimension (cm)
5.6819	5.6671	14.8	0.0213	2.0 mol·dm^{-3}	2.3×1.2×0.1
5.6737	5.6632	10.5	0.0151	1.5 mol·dm^{-3}	2.3×1.2×0.1
5.6682	5.6598	8.4	0.0121	1.0 mol·dm^{-3}	2.3×1.2×0.1
5.5955	5.5948	7.0	0.01	0.5 mol·dm^{-3}	2.3×1.2×0.1

Table 4S. Copper samples immersed in different concentrations of H_2SO_4 solution at 55°C for 15.0 hours.

Weight of copper piece (g)	Weight after immersed in H_2SO_4 (g)	Δ*w* (mg)	Corrosion rate g/cm^2·h	Concentration of H_2SO_4 solution	Dimension (cm)
5.8835	5.8576	25.9	0.0373	2.0 mol·dm^{-3}	2.3×1.2×0.1
5.8220	5.7995	22.5	0.0323	1.5 mol·dm^{-3}	2.3×1.2×0.1
5.8068	5.7877	19.1	0.0275	1.0 mol·dm^{-3}	2.3×1.2×0.1
5.7714	5.7698	16.0	0.023	0.5 mol·dm^{-3}	2.3×1.2×0.1

Table 5S. Copper samples immersed in 2.0 mol·dm^{-3} of H_2SO_4 solution for 15 hours in the presence of PEG 400 at 25°C.

Conc. of PEG 400	Δ*w* (g)	Corrosion rate g/cm^2·h	Concentration of H_2SO_4 solution	Dimension (cm)
0.000077 M	6.3	0.00907	2.0 mol·dm^{-3}	2.3×1.2×0.1
0.000153 M	5.3	0.00767	2.0 mol·dm^{-3}	2.3×1.2×0.1
0.00023 M	4.6	0.00662	2.0 mol·dm^{-3}	2.3×1.2×0.1
0.000307 M	4.0	0.00576	2.0 mol·dm^{-3}	2.3×1.2×0.1

Table 6S. Copper samples immersed in in 2.0 mol·dm^{-3} of H_2SO_4 solution for 15 hours in the presence of PEG 4000 at 25°C.

Conc. of PEG 4000	Δ*w* (g)	Corrosion rate g/cm^2·h	Concentration of H_2SO_4 solution	Dimension (cm)
0.000077 M	4.6	0.00662	2.0 mol·dm^{-3}	2.3×1.2×0.1
0.000153 M	3.2	0.00454	2.0 mol·dm^{-3}	2.3×1.2×0.1
0.00023 M	1.9	0.00273	2.0 mol·dm^{-3}	2.3×1.2×0.1
0.000307 M	1.3	0.00187	2.0 mol·dm^{-3}	2.3×1.2×0.1

Table 7S. Copper samples immersed in in 2.0 mol·dm^{-3} of H_2SO_4 solution for 15 hours in the presence of PVP k15 at 25°C.

Conc. of PVP k15	Δ*w* (g)	Corrosion rate g/cm^2·h	Concentration of H_2SO_4 solution	Dimension (cm)
0.000077 M	4.1	0.00590	2.0 mol·dm^{-3}	2.3×1.2×0.1
0.000153 M	2.7	0.00392	2.0 mol·dm^{-3}	2.3×1.2×0.1
0.00023 M	1.6	0.00230	2.0 mol·dm^{-3}	2.3×1.2×0.1
0.000307 M	0.7	0.001	2.0 mol·dm^{-3}	2.3×1.2×0.1

Table 8S. Copper samples immersed in in 2.0 mol·dm^{-3} of H_2SO_4 solution for 15 hours in the presence of PEG 400 at 35°C.

Conc. of PEG 400	Δ*w* (g)	Corrosion rate g/cm^2·h	Concentration of H_2SO_4 solution	Dimension (cm)
0.000077 M	9.6	0.0137	2.0 mol·dm^{-3}	2.3×1.2×0.1
0.000153 M	8.6	0.0124	2.0 mol·dm^{-3}	2.3×1.2×0.1
0.00023 M	7.8	0.0112	2.0 mol·dm^{-3}	2.3×1.2×0.1
0.000307 M	7.0	0.0101	2.0 mol·dm^{-3}	2.3×1.2×0.1

Table 9S. Copper samples immersed in in 2.0 mol·dm^{-3} of H_2SO_4 solution for 15 hours in the presence of PEG 4000 at 35°C.

Conc. of PEG 4000	Δ*w* (g)	Corrosion rate g/cm^2·h	Concentration of H_2SO_4 solution	Dimension (cm)
0.000077 M	8.7	0.0125	2.0 mol·dm^{-3}	2.3×1.2×0.1
0.000153 M	7.5	0.0108	2.0 mol·dm^{-3}	2.3×1.2×0.1
0.00023 M	6.5	0.00936	2.0 mol·dm^{-3}	2.3×1.2×0.1
0.000307 M	5.1	0.00734	2.0 mol·dm^{-3}	2.3×1.2×0.1

Table 10S. Copper samples immersed in in 2.0 mol·dm^{-3} of H_2SO_4 solution for 15 hours in the presence of PVP k15 at 35°C.

Conc. of PVP k15	Δ*w* (g)	Corrosion rate g/cm^2·h	Concentration of H_2SO_4 solution	Dimension (cm)
0.000077 M	7.5	0.0108	2.0 mol·dm^{-3}	2.3×1.2×0.1
0.000153 M	5.8	0.00835	2.0 mol·dm^{-3}	2.3×1.2×0.1
0.00023 M	4.5	0.00648	2.0 mol·dm^{-3}	2.3×1.2×0.1
0.000307 M	3.2	0.00461	2.0 mol·dm^{-3}	2.3×1.2×0.1

Table 11S. Copper samples immersed in in 2.0 mol·dm^{-3} of H_2SO_4 solution for 15 hours in the presence of PEG 400 at 45°C.

Conc. of PEG 400	Δ*w* (g)	Corrosion rate g/cm^2·h	Concentration of H_2SO_4 solution	Dimension (cm)
0.000077 M	14.3	0.0206	2.0 mol·dm^{-3}	2.3×1.2×0.1
0.000153 M	13.4	0.0193	2.0 mol·dm^{-3}	2.3×1.2×0.1
0.00023 M	12.8	0.0184	2.0 mol·dm^{-3}	2.3×1.2×0.1
0.000307 M	12.2	0.0176	2.0 mol·dm^{-3}	2.3×1.2×0.1

Table 12S. Copper samples immersed in in 2.0 mol·dm^{-3} of H_2SO_4 solution for 15 hours in the presence of PEG 4000 at 45°C.

Conc. of PEG 4000	Δ*w* (g)	Corrosion rate g/cm^2·h	Concentration of H_2SO_4 solution	Dimension (cm)
0.000077 M	13.1	0.0189	2.0 mol·dm^{-3}	2.3×1.2×0.1
0.000153 M	12.2	0.0175	2.0 mol·dm^{-3}	2.3×1.2×0.1
0.00023 M	11.8	0.0170	2.0 mol·dm^{-3}	2.3×1.2×0.1
0.000307	11.0	0.0159	2.0 mol·dm^{-3}	2.3×1.2×0.1

Table 13S. Copper samples immersed in in 2.0 mol·dm^{-3} of H_2SO_4 solution for 15 hours in the presence of PVP k15 at 45°C.

Conc. of PVP k15	Δ*w* (g)	Corrosion rate g/cm^2·h	Concentration of H_2SO_4 solution	Dimension (cm)
0.000077 M	11.5	0.0165	2.0 mol·dm^{-3}	2.3×1.2×0.1
0.000153 M	10.0	0.0144	2.0 mol·dm^{-3}	2.3×1.2×0.1
0.00023 M	8.6	0.0123	2.0 mol·dm^{-3}	2.3×1.2×0.1
0.000307 M	7.7	0.011	2.0 mol·dm^{-3}	2.3×1.2×0.1

Table 14S. Copper samples immersed in in 2.0 mol·dm^{-3} of H_2SO_4 solution for 15 hours in the presence of PEG 400 at 55°C.

Conc. of PEG 400	Δ*w* (g)	Corrosion rate g/cm^2·h	Concentration of H_2SO_4 solution	Dimension (cm)
0.000077 M	25.3	0.0364	2.0 mol·dm^{-3}	2.3×1.2×0.1
0.000153 M	24.2	0.0348	2.0 mol·dm^{-3}	2.3×1.2×0.1
0.00023 M	23.0	0.0331	2.0 mol·dm^{-3}	2.3×1.2×0.1
0.000307 M	22.2	0.0320	2.0 mol·dm^{-3}	2.3×1.2×0.1

Table 15S. Copper samples immersed in in 2.0 mol·dm^{-3} of H_2SO_4 solution for 15 hours in the presence of PEG 4000 at 55°C.

Conc. of PEG 4000	Δ*w* (g)	Corrosion rate g/cm^2·h	Concentration of H_2SO_4 solution	Dimension (cm)
0.000077 M	24.0	0.0347	2.0 mol·dm^{-3}	2.3×1.2×0.1
0.000153 M	23.1	0.0332	2.0 mol·dm^{-3}	2.3×1.2×0.1
0.00023 M	21.9	0.0315	2.0 mol·dm^{-3}	2.3×1.2×0.1
0.000307 M	21.4	0.0308	2.0 mol·dm^{-3}	2.3×1.2×0.1

Table 16S. Copper samples immersed in in 2.0 mol·dm^{-3} of H_2SO_4 solution for 15 hours in the presence of PVP k15 at 55°C.

Conc. of PVP k15	Δ*w* (g)	Corrosion rate g/cm^2·h	Concentration of H_2SO_4 solution	Dimension (cm)
0.000077 M	22.4	0.0322	2.0 mol·dm^{-3}	2.3×1.2×0.1
0.000153 M	20.2	0.0291	2.0 mol·dm^{-3}	2.3×1.2×0.1
0.00023 M	19.1	0.0275	2.0 mol·dm^{-3}	2.3×1.2×0.1
0.000307	17.8	0.0256	2.0 mol·dm^{-3}	2.3×1.2×0.1

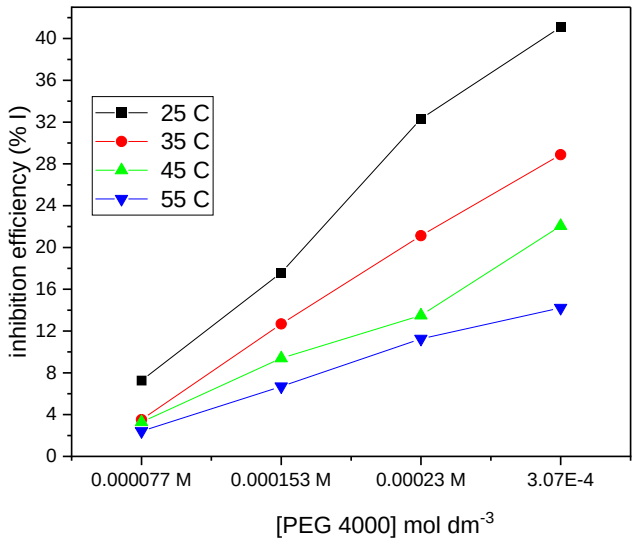

Figure 1S. Plot of inhibition efficiency (%*I*) against inhibitor concentration for copper in 2.0 mol·dm^{-3} H_2SO_4 solution containing PEG 400 at different temperatures.

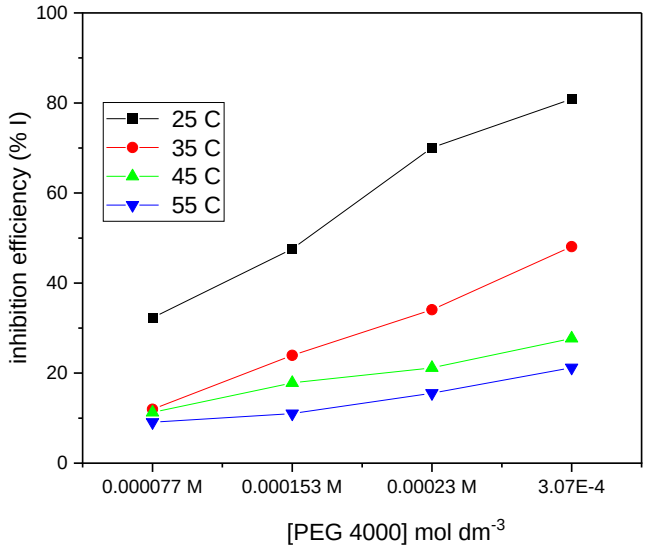

Figure 2S. Plot of inhibition efficiency (%*I*) against inhibitor concentration for copper in 2.0 mol·dm^{-3} H_2SO_4 solution containing PEG 4000 at different temperatures.

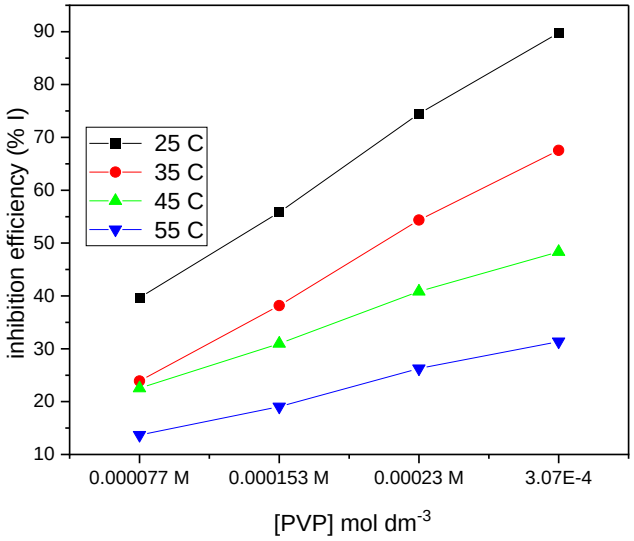

Figure 3S. Plot of inhibition efficiency (%*I*) against inhibitor concentration for copper in 2.0 M H_2SO_4 solution containing PVP k15 at different temperatures.

♦ ♦ ♦